JETIR.ORG ISSN: 2349-5162 | ESTD Year : 2014 | Monthly Issue
JOURNAL OF EMERGING TECHNOLOGIES AND INNOVATIVE RESEARCH (JETIR)
An International Scholarly Open Access, Peer-reviewed, Refereed Journal

A COMPARATIVE ANALYSIS OF HISTOGRAM EQUALIZATION BASED CONTRAST ENHANCEMENT TECHNIQUES FOR CHEST-X RAY (CXR) IMAGES

Ekta, Reeta Devi✉
Department of Electronics and Communication Engineering
University Institute of Engineering and Technology, Kurukshetra University, Kurukshetra, Haryana, India - 136119

ABSTRACT: In the pandemic time due to Covid-19, researchers are searching for alternative screening methods to prevent outbreaks. Therefore, chest X-ray (CXR) imaging is being explored worldwide because of its several benefits, such as being cheaper and easy to deploy in rural and remote areas. However, CXR images may result in low contrast due to various machine-oriented internal factors and environmental triggered external factors. Hence, there is an urgent need to study different contrast enhancement techniques for CXR images, as they significantly influence both human perception and computer vision. Histogram Equalization is a prominent technique for enhancing contrast in image processing that utilizes the histogram of an image. However, its effectiveness is limited because it often causes a significant difference in mean brightness between the output and input images. To address the challenge of preserving brightness, several extensions of histogram equalization have been proposed. Notably, adaptive histogram equalization (AHE), contrast limited adaptive histogram equalization (CLAHE), brightness preserving bi-histogram equalization (BBHE), dualistic sub-image histogram equalization (DSIHE), recursive mean-shift histogram equalization (RMSHE), recursive sub-image histogram equalization (RSIHE), minimum mean brightness error bi-histogram equalization (MMBEBHE), and recursively separated and weighted histogram equalization (RSWHE) have been suggested by various researchers. This paper provides a comprehensive review of these popular histogram equalization techniques as an experimental study on CXR images and evaluates their performance using metrics such as Peak Signal-to-Noise Ratio (PSNR), Absolute Mean Brightness Error (AMBE), and Structural Similarity Index (SSI).

***Index Terms**:* Contrast Enhancement, Covid-19, CXR, Histogram Equalization, HE variants.

I. INTRODUCTION

The SARS-CoV-2 outbreak, known as COVID-19, began in Wuhan, China, in December 2019. By February 26, 2020, it had spread to every continent except Antarctica, with 3.53 million confirmed cases and 248,169 deaths reported across 210 countries by May 4, 2020 [1], [2]. Initially, India had lower case counts and deaths compared to many developed nations, but by the end of June 2020, it became the third-most affected country. This surge resulted in critical shortages of hospital beds, ventilators, and medical staff, leading to a sharp increase in fatalities [3]. To counter the virus's spread, rapid and reliable diagnosis is essential. Current tests, such as reverse transcriptase polymerase chain reaction (RT-PCR), Real-time RT-PCR (rRT-PCR) and Reverse transcription loop-mediated isothermal amplification (RT-LAMP) can take up to two days for results, causing delays and increasing the risk of false negatives [1], [4]. To address these issues, innovative approaches using artificial intelligence in medical imaging, like computed tomography (CT) and chest X-rays (CXR), are being explored [5]. These methods provide quicker and more accessible diagnostics, enabling timely treatment and ultimately saving lives while reducing the impact of SARS-CoV-2.

Since the emergence of COVID-19, numerous studies have employed deep learning for automated detection using chest X-rays [3], [6], [7], [8], [9]. However, this approach has not yet become part of standard clinical practice due to limited generalization [10], [11], [12]. The main challenges are technological limitations and the poor quality of images affected by various machine-oriented internal factors and environmental-triggered external factors [13], [14]. Low-dose chest X-rays often produce images with low contrast [15]. Furthermore, improper setup of X-ray imaging devices—such as source-to-image receptor distance, orientation, magnification, and focal spot size—frequently leads to images with uneven illumination [13], [15]. These non-uniform images may show overexposed, underexposed, or well-exposed areas [16]. Research on automated COVID-19 detection from chest X-rays rarely discusses enhancement techniques used during preprocessing and tends to apply the same global enhancement method to the entire image [6], [7], [9], [12], [13]. Global enhancement can either over-enhance or under-enhance non-uniform illumination, potentially impairing accurate COVID-19 diagnosis.

Therefore, there is an urgent need to study different contrast enhancement techniques for CXR images, as it significantly influences both human perception and computer vision. A prominent method is histogram equalization (HE), which aims to evenly distribute pixel intensities throughout the image [17]. However, it confronts the "mean-shift" problem, which can negatively impact brightness preservation [16]. To tackle this issue, researchers introduced adaptive histogram equalization (AHE) and contrast limited adapted histogram equalization [18], while Yeong-Taeg Kim developed brightness preserving histogram equalization (BBHE) [19]. BBHE enhances two distinct intensity ranges by splitting the histogram at the mean value, providing a more tailored approach. Further advancements include dualistic sub-image histogram equalization (DSIHE) by Yu Wan and colleagues [20], which enhances brightness preservation through a cumulative probability density of 0.5. Additionally, recursive mean-shift histogram equalization (RMSHE) [21] builds on BBHE's foundation by recursively refining the histogram to align the output image's brightness more closely with the original, and recursive sub-image histogram equalization (RSIHE) extends DSIHE by separating the input histogram based on a cumulative distribution function equal to 0.5 [22]. Moreover, the Minimum Mean Brightness Error Bi-Histogram Equalization (MMBEBHE) [23] devised by Chen and Ramil focuses on maximizing brightness preservation by minimizing errors effectively. Lastly, Mary Kim and Min Gyo Chung introduced the Recursively Separated and Weighted Histogram Equalization (RSWHE) [24], which segments the input histogram and implements a distinctive weighting process, resulting in significant improvements over previous methods. The progression in this field is truly remarkable. A detailed study on these algorithms are presented in subsequent sections of this article.

This manuscript is prepared to examine the comparative effects of contrast enhancement on CXR images using histogram equalization and its variants such as AHE, CLAHE, BBHE, DSIHE, RSIHE, RMSHE, MMBEBHE, and RSWHE as discussed above. The rest of the article is structured as follows: Section II describes contrast enhancement techniques like HE, BBHE, and DSIHE. Section III discusses other variants of HE. Results and discussion are presented in Section IV. Finally, Section V concludes the article.

II. CONTRAST ENHANCEMENT TECHNIQUES

2.1 Histogram Equalization

Histogram equalization is a technique used in image processing to enhance the contrast of an image by redistributing the intensity values across the entire range. It works by spreading out the most frequent intensity values, which can improve the visual quality of images, especially those with poor contrast as shown in the Figure 1 which shows Covid-19 positive CXR images having low contrast downloaded from Kaggle. Figure 2 shows the histogram plots of these images. The more common variants of HE, AHE works on small regions of the image for better local contrast and Clip Limited AHE limits contrast amplification to reduce noise [18].

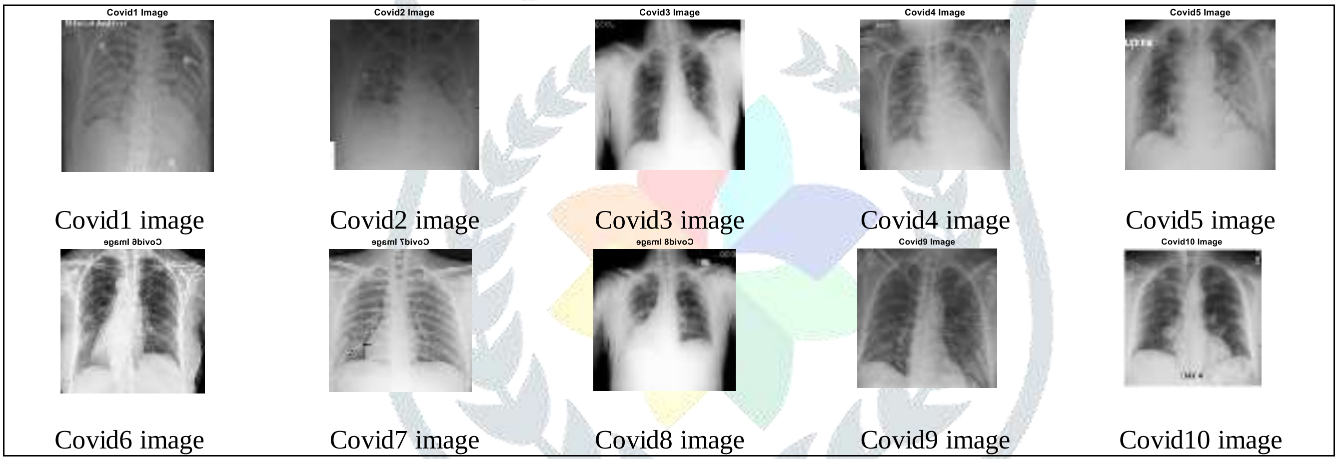

Figure 1: Low contrast Covid-19 positive CXR images.

A. Mathematical Formulation of the Histogram Equalization

Lets consider a discrete grayscale input image $A = a(i,j)$, with the L discrete levels, where $a(i,j)$ denotes the intensity levels of the image at the spatial domain (i,j). Let Histogram of the input image $H(A)$. Now, the probability density function $pdf(A)$ is defined as:

$$pdf(A_k) \text{ or } p(A_k) = {m_k}/{N} \qquad (1)$$

where, $0 \leq k \leq L-1$

L is the number of gray levels in the image,

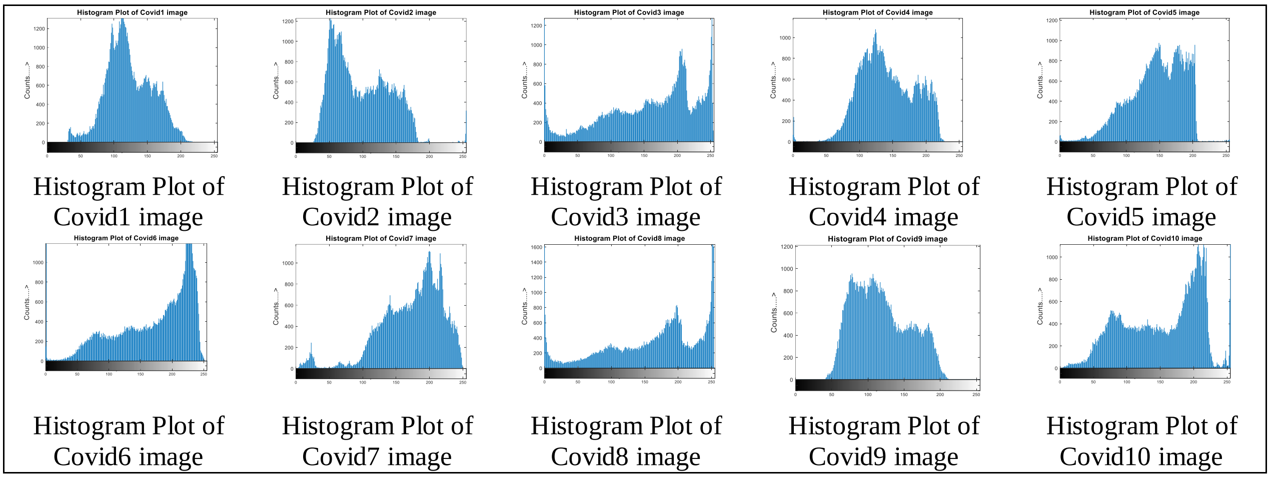

Histogram Plot of Covid1 image | Histogram Plot of Covid2 image | Histogram Plot of Covid3 image | Histogram Plot of Covid4 image | Histogram Plot of Covid5 image

Histogram Plot of Covid6 image | Histogram Plot of Covid7 image | Histogram Plot of Covid8 image | Histogram Plot of Covid9 image | Histogram Plot of Covid10 image

Figure 2: Histogram plots of CXR images shown in Figure 1.

N is the total number of pixels in the image,

m_k is the total number of pixels with the same intensity level k.

From the $pdf(A_k)$ as defined in equation (1), cumulative distribution function $cdf(A_i)$ defined as-

$$cdf(A_i) \text{ or } c(A_i) = \sum_{i=0}^{k} p(A_i) \tag{2}$$

From equations (1) and (2), $cdf(A_{L-1}) = 1$.

Histogram equalisation is a technique that maps the input image into the entire dynamic range $[A0, A_{L-1}]$ by using the cumulative distribution function as a transform function. Now, the transform function $T(A)$ using the cumulative distribution function $cdf(A_i)$ as-

$$T(A) = A_0 + (A_{L-1} - A_0) \times cdf(A_i) \tag{3}$$

Then the output image of histogram equalization, $B = b(i,j)$ can be expressed as

$$B = T(A) \tag{4}$$

$$B = \{T(a(i,j)) | \forall\, a(i,j) \in A\} \tag{5}$$

The above describe the histogram equalization on gray scale image. However it can also be used on color image by applying the same method separately to the red, green and blue components of the RGB image.

2.2 Brightness Preserving Bi-Histogram Equalisation (BBHE)

The BBHE [19] firstly decomposes an input image histogram $H(A)$ into two sub-images by using mean of the input image. Let us consider A_L and A_U as the two sub-images of the input image obtained with the help of mean value A_{mean}, where $A_{mean} \in \{A_0, A_1 \ldots\ldots A_{L-1}\}$ such that

$$\mathrm{A} = \mathrm{A_L} \cup \mathrm{A_U} \tag{6}$$

where

$$A_L = \{a(i,j) | a(i,j) \le A_{mean} \forall\, a(i,j) \in A\} \tag{7}$$

and

$$A_U = \{a(i,j) | a(i,j) > A_{mean} \forall\, a(i,j) \in A\} \tag{8}$$

And mean of the input image is calculated by,

$$A_{mean} = \frac{(\sum_{i=0}^{i=L-1} ip(A_i))}{(\sum_{i=0}^{i=L-1} p(A_i))} \tag{9}$$

It is evident that the sub-image A_L is composed of $\{A_0, A_1 \ldots\ldots A_m\}$ and the sub-image A_U is composed of $\{A_{m+1}, A_{m+2} \ldots\ldots A_{L-1}\}$.

Now, the probability density function (pdf) of the sub-images A_L and A_U are:

$$pdf_L(A_k) \text{ or } p_L(A_k) = {}^{m_k}/_{N_L} \tag{10}$$

where, k = 0,1,2,…..m.

and

$pdf_U(A_k)$ or $p_U(A_k) = {}^{m_k}/_{N_U}$ (11)

where, k = m+1, m+2,…….L-1.

Here N_L and N_U represents the total number of pixels in the sub-images A_L and A_U respectively. The respective cumulative distribution function (cdf) is:

$$cdf_L(A_i) = \sum_{i=0}^{m} P_L(A_i) \quad (12)$$

and

$$cdf_U(A_i) = \sum_{i=m+1}^{L-1} P_U(A_i) \quad (13)$$

Now, defining transformation function for each sub-image;

$$T_L(A_L) = A_0 + (A_m - A_0) \times cdf_L(A_i) \quad (14)$$

and

$$T_U(A_U) = A_{m+1} + (A_{L-1} - A_{m+1}) \times cdf_U(A_i) \quad (15)$$

Equations (14) and (15) define the transformed sub-images. Now the output of BBHE is obtained as:

$B_{BBHE} = B_{BBHE}(I,J)$

$= T_L(A_L) \cup T_U(A_U)$ (16)

where

$$T_L(A_L) = T_L\{a(i,j)|a(i,j) \le A_{mean} \forall\, a(i,j) \in A\} \quad (17)$$

and

$$T_U(A_U) = T_U\{a(i,j)|a(i,j) > A_{mean} \forall\, a(i,j) \in A\} \quad (18)$$

$T_L(A_L)$ equalize the sub-image A_L over the range $\{A_0, A_m\}$ and $T_U(A_U)$ equalize the sub-image A_U over the range $\{A_{m+1}, A_{L-1}\}$.

2.3 Equal Area Dualistic Sub-Image Histogram Equalization (DSIHE)

Equal area dualistic sub-image histogram equalization (DSIHE) [20] method decomposes the input image based on the gray levels with a cumulative distribution value equals to 0.5 unlike the mean value in BBHE method. DSIHE method decomposes the original image aiming at maximizing the Shannon's entropy of the output image. For such aim, the input image is decomposed into two sub-images being one dark and one bright, and then applies the HE on the decomposed sub-images. Then compose the resultant histogram equilized sub-images into one image to produce the DSIHE output image. Considering R_{med} as the median value which divides the original input image $R(i,j)$ into two parts R_L and R_U such that

$$R = R_L \cup R_U \quad (19)$$

where

$$R_L = \{r(i,j)|r(i,j) \le R_{med} \ \forall\, r(i,j) \in R\} \quad (20)$$

and

$$R_U = \{r(i,j)|r(i,j) > R_{med} \ \forall\, r(i,j) \in R\} \quad (21)$$

and

$$R_{med} = argMin_{0 \le k \le L-1} \left| cdf(R_k) - \frac{cdf(R_0)+cdf(R_{L-1})}{2} \right| \quad (22)$$

where sub-image R_L is composed by the $\{R_0, R_1 \dots \dots R_{h-1}\}$ and the sub-image R_U is composed by the $\{R_h, R_{h+1} \dots \dots R_{L-1}\}$.

Now the probability density functions $pdf_L(R_k)$ or $p_L(R_k)$ and $pdf_U(R_k)$ or $p_U(R_k)$ of the sub-images R_L and R_U respectively, are defined as:

$pdf_L(R_k)$ or $p_L(R_k) = {}^{m_k}/_{N_L}$; where k=1,2,3,……h-1 (23)

and

$pdf_L(R_k)$ or $p_L(R_k) = {}^{m_k}/_{N_L}$; where k=h,h+1,h+2,……L-1 (24)

Cumulative distribution function for both sub-images R_L and R_U is computed as:

$$cdf_L(R_k) = \sum_{i=0}^{h-1} p_L(R_k) \quad (25)$$

and

$$cdf_U(R_k) = \sum_{i=h}^{L-1} p_U(R_k) \quad (26)$$

Now, the transformation function is defined as:

$$T_L(R_L) = R_0 + (R_{h-1} - R_0)cdf_L(R_k) \quad (27)$$

and

$$T_U(R_U) = R_h + (R_{L-1} - R_h)cdf_U(R_k) \quad (28)$$

Finally, the output image is

$B_{DSIHE} = B_{DSIHE}(I,J)$

$$= T_L(R_L) \cup T_U(R_U) \quad (29)$$

where

$$T_L(R_L) = T_L\{r(i,j)|r(i,j) \le R_{med} \forall\, r(i,j) \in R\} \quad (30)$$

and

$$T_U(R_U) = T_U\{r(i,j)|r(i,j) > R_{med} \forall\, r(i,j) \in R\} \quad (31)$$

$T_L(R_L)$ equalize the sub-image R_L over the range $\{R_0, R_{h-1}\}$ and $T_U(R_U)$ equalize the sub-image R_U over the range $\{R_h, R_{L-1}\}$.

III. OTHER VARIANTS OF HISTOGRAM EQUALIZATION (RMSHE, RSIHE, MMBEBHE, RSWHE)

The Recursive Mean Separate Histogram Equalization (RMSHE) [21] method significantly advances the Brightness Preserving Bi-Histogram Equalization (BBHE) technique by employing a recursive strategy for histogram separation. Unlike BBHE, which merely divides the histogram into two segments at the mean, RMSHE enhances this process by continuously partitioning each resulting histogram according to their respective means. This recursive approach greatly enhances the ability to preserve brightness at multiple levels, making RMSHE exceptionally effective for consumer electronic devices where image quality is paramount. By enabling scalable preservation, RMSHE not only improves the contrast of images but also effectively addresses the mean-shift problem that often limits traditional histogram equalization methods. This ensures that users receive clearer and more accurate images, crucial for a range of applications in today's technology-driven world.

Recursive sub-image histogram equalization (RSIHE) [22] is an effective contrast enhancement technique that advances the dualistic sub-image histogram equalization (DSIHE) method. By employing a cumulative probability density of 0.5, RSIHE divides the input histogram into sub-histograms, enabling recursive application across multiple levels. This approach results in uniformly sized sub-images, each containing an equal number of pixels. A significant advantage of RSIHE is its capability to preserve brightness while enhancing contrast, which is particularly crucial for chest X-ray (CXR) images where accurate diagnosis relies on consistent luminance. As such, RSIHE presents a compelling solution for enhancing the clarity of vital diagnostic images.

Minimum Mean Brightness Error Bi-Histogram Equalization (MMBEBHE) [23] is an enhancement technique derived from Brightness Preserving Bi-Histogram Equalization (BBHE). This approach segments the histogram using a threshold that minimizes the Absolute Mean Brightness Error (AMBE). Initially, MMBEBHE calculates the AMBE for various thresholds and identifies the optimal threshold, denoted as T1, which results in the smallest mean brightness error. The histogram is then divided at this threshold, and histogram equalization is conducted separately on each segment, similar to the BBHE methodology.

On the other hand, Recursively Separated and Weighted Histogram Equalization (RSWHE) [24] is a later technique designed to enhance image contrast while maintaining brightness. RSWHE comprises three key components: histogram segmentation, histogram weighting, and histogram equalization. The histogram segmentation element partitions the input image histogram, similar to approaches used in Recursive Mean-Shift Histogram Equalization (RMSHE) or Recursive Sub-Image Histogram Equalization (RSIHE). This process involves recursively dividing the input histogram H(A) to a specified recursion level, employing two methods: one based on the mean and the other on the median of the resulting sub-histograms. This dual approach aims to achieve better contrast enhancement without altering the overall brightness of the image.

After histogram segmentation with a recursion level of x, the 2^x number of sub-histograms will be generated, i.e. $H_i^x(A), \{1 \le i \le 2^x\}$. Then, the histogram weighting module specially modifies the probability density function of each sub histogram using the normalized power law function.

For each sub-histogram $H_i^x(A)$, corresponding original pdf $p(A_k)$, the weighted pdf $p_w(A_k)$ is described as follows:

$$p_w(A_k) = p_{max}\left(\frac{p(A_k) - p_{min}}{p_{max} - p_{min}}\right)^{C_i} + \emptyset, \ (L_i \le k \le U_i) \quad (32)$$

where, p_{max} and p_{min} are maximum and minimum probability values from original histogram respectively. C_i is an accumulative probability value for i[th] sub-histogram $H_i^x(A)$. C_i is calculated for each sub-histogram.

$$C_i = \sum_{K=L_i}^{U_i} p(A_k) \quad (33)$$

and $\emptyset$ is a value which is greater than 0. The degree of mean brightness and contrast enhancement of output image can be controlled by adjusting $\emptyset$ which can be found experimentally by using the formula given in Equation (34).

$$\emptyset = p_{max}\left(|A_M - A_G| \big/ (A_{max} - A_{min})\right) \quad (34)$$

where A_{max} and A_{min} are the greatest and lowest values of gray levels in the input image A. After the weighting process, normalization is necessary to adjust the weighted histogram. Each sub-histogram's weighted and normalized PDF is then histogram equalized individually. Finally, all the resulting sub-images are combined to produce the output of the RSWHE method.

IV. RESULTS AND DISCUSSION

We processed numerous low-contrast images to demonstrate the effectiveness of various histogram equalization methods discussed earlier. From Kaggle, we selected ten Covid-19 positive CXR images with low contrast, as shown in Figure 1 (Covid1-Covid10 CXR images), and applied HE, AHE, CLAHE, BBHE, DSIHE, RMSHE, RSIHE, MMBEBHE, and RSWHE techniques to evaluate their performance. A specific low-contrast Covid-19 positive CXR image (Covid1 image) along with its histogram plot is shown below in Figure 3. It has been enhanced by variants of HE as discussed above, and the resulting contrast-enhanced images with their histogram plots are shown in Figure 4. The quantitative assessment of all these methods was performed using metrics such as peak signal-to-noise ratio (PSNR), absolute mean brightness error (AMBE), and structural similarity index measure (SSIM), as shown in Tables 1-3, respectively.

The results in Table 1 clearly demonstrate the PSNR (Peak Signal-to-Noise Ratio) values for various methods applied to CXR images, underscoring PSNR as a crucial metric for image quality assessment. Higher PSNR values indicate superior image quality. It’s apparent from Table 1 that RSWHE by mean method achieves the highest PSNR values for the images, boasting an average PSNR that surpasses all other histogram equalization methods. Notably, RMSHE ranks a solid second, delivering promising results.

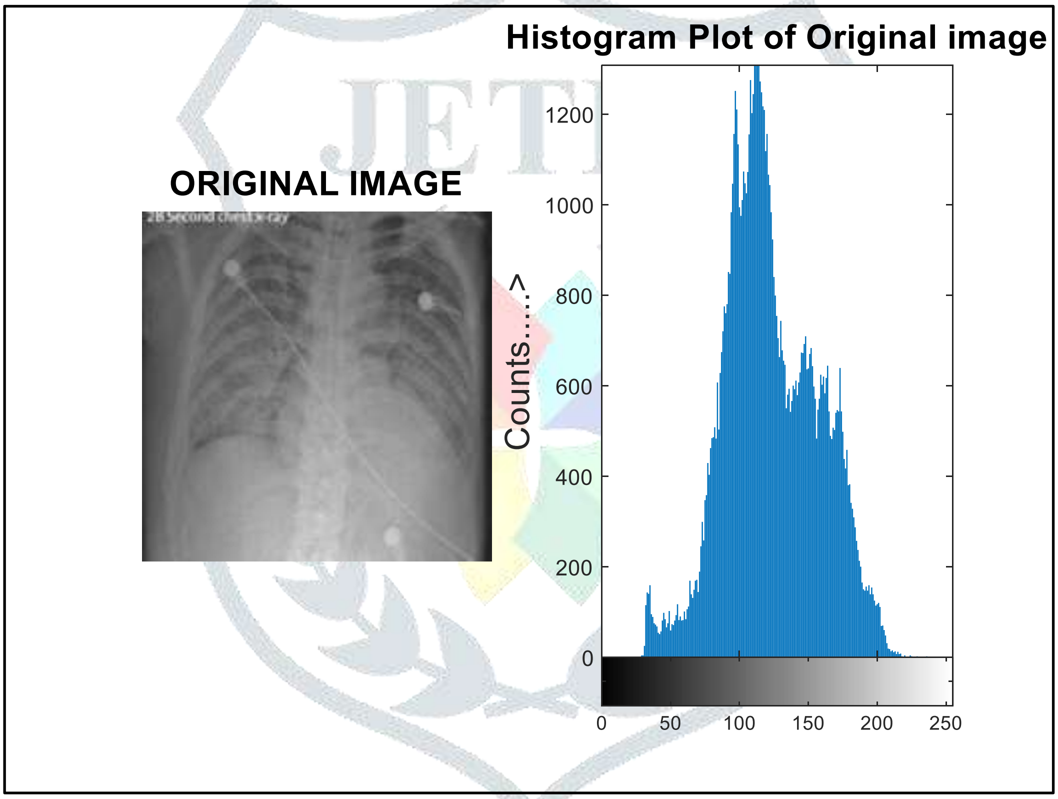

Figure 3: Low Contrast Original Covid-19 positive (Covid1) CXR image

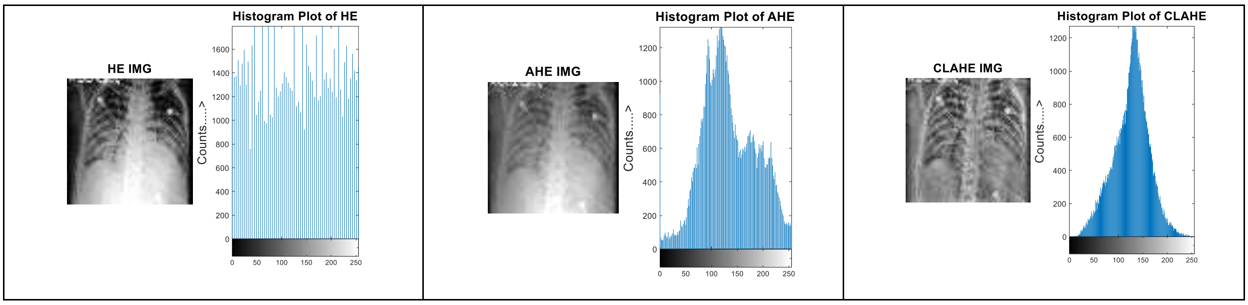

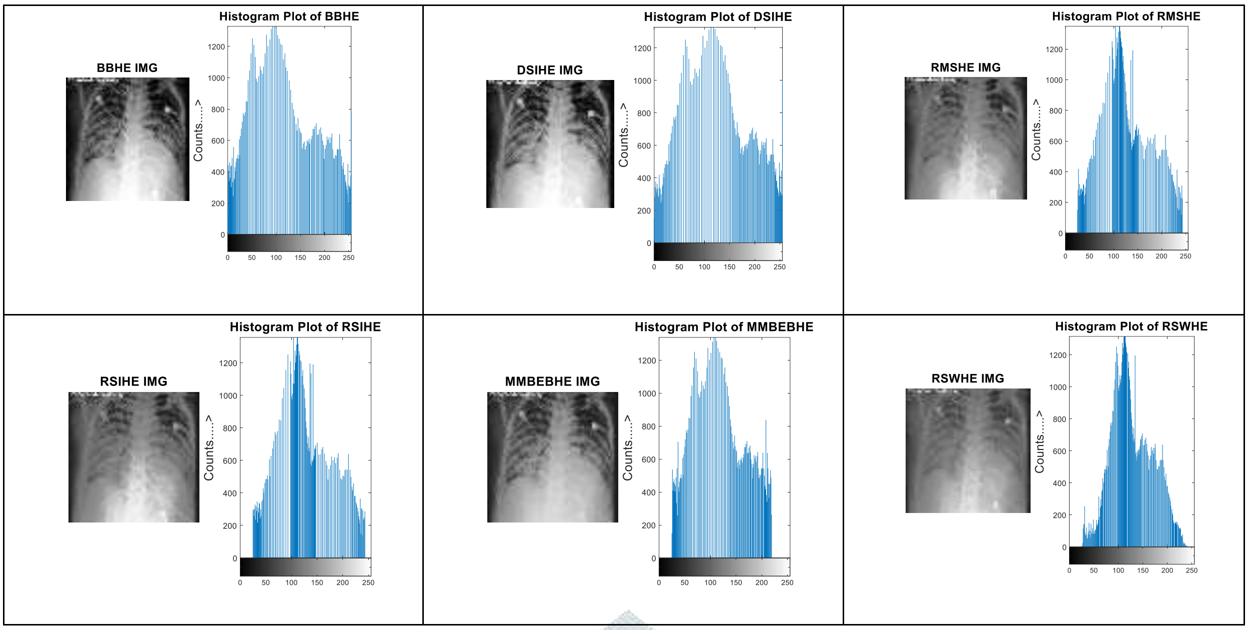

Figure 4: Contrast Enhanced COVID-19 CXR image by applying HE, AHE, CLAHE, BBHE, DSIHE, RMSHE, RSIHE, MMBEBHE, and RSWHE techniques

Table 1: Peak Signal to Noise Ratio (PSNR) of all Methods

Covid image	HE	AHE	CLAHE	BBHE	DSIHE	RMSHE	RSIHE	MMBEBHE	RSWHE
Covid1	15.59238	15.59238	18.52917	15.88112	15.59382	23.19682	22.45128	20.64349	29.97955
Covid2	14.92504	14.92504	18.56466	17.21438	13.99946	21.63408	21.00879	23.47411	26.34731
Covid3	18.29299	18.29299	15.72408	29.01856	17.04121	29.17142	29.81201	26.0419	44.85918
Covid4	16.48454	16.48454	17.75738	16.86263	17.39969	22.16034	21.93952	20.18168	31.62834
Covid5	15.8638	15.8638	19.00243	17.15487	16.85336	21.6024	21.19123	19.66509	29.49498
Covid6	13.94964	13.94964	13.84738	23.25694	15.69135	28.6806	26.78645	22.02416	35.32983
Covid7	12.85877	12.85877	14.48845	17.35284	14.50831	24.45448	21.07515	27.18336	32.57045
Covid8	18.83067	18.83067	16.17212	25.72885	16.76831	25.59992	25.47318	22.96735	46.07616
Covid9	16.44559	16.44559	18.03737	17.05345	15.51699	30.89779	30.93341	25.27068	39.23297
Covid10	17.98838	17.98838	15.88422	22.72528	18.37229	24.75797	24.84196	27.00614	34.36539
Mean Value	16.1232	16.1231	16.8007	20.2248	16.1745	25.2156	24.5513	23.4458	**34.9884**

Table 2: Absolute Mean Brightness Error (AMBE) of all Methods

Covid image	HE	AHE	CLAHE	BBHE	DSIHE	RMSHE	RSIHE	MMBEBHE	RSWHE
Covid1	4.580128	11.61345	3.12737	2.921444	9.436192	1.786177	2.801568	0.012148	2.222268
Covid2	29.66083	11.89837	15.36624	11.17015	40.32397	6.954743	8.378173	3.650731	4.748336
Covid3	25.01483	1.796065	23.36786	0.791378	30.26955	2.101028	0.467176	2.10303	0.470834
Covid4	13.8276	7.19228	11.43199	10.25853	1.522097	6.935459	7.248756	0.139126	2.069216
Covid5	17.81943	18.56129	10.11475	1.076878	5.21502	1.748247	1.168208	0.028915	0.520005
Covid6	44.37111	8.160267	39.61686	8.380566	32.55426	2.084071	3.87744	10.93544	1.39117
Covid7	46.29228	1.330075	37.71554	12.64137	31.02474	4.069384	8.41919	2.284751	2.081118
Covid8	21.03473	1.211161	19.81356	3.456539	31.07837	1.2989	2.825192	0.006163	0.293364
Covid9	9.488675	4.675921	5.220915	0.529737	29.13105	0.230109	0.512041	0.134216	0.384078
Covid10	24.74994	14.10531	20.67369	5.20162	23.407	2.478227	3.119551	1.086073	0.894587
Mean Value	23.6839	8.0544	18.6448	5.6428	23.3962	2.9686	3.8817	2.0380	**1.5075**

Table 3: Structure Similarity Index (SSIM) of all Methods

Covid image	HE	AHE	CLAHE	BBHE	DSIHE	RMSHE	RSIHE	MMBEBHE	RSWHE
Covid1	0.731367	0.94512	0.671123	0.751697	0.74935	0.922282	0.916363	0.869293	0.986707
Covid2	0.834118	0.903115	0.784547	0.87414	0.855846	0.964754	0.964628	0.938725	0.989844
Covid3	0.859193	0.9997	0.742863	0.918334	0.880744	0.923933	0.923917	0.85085	0.980747
Covid4	0.780016	0.919438	0.712834	0.80043	0.814557	0.89417	0.890175	0.808186	0.982596
Covid5	0.777386	0.942462	0.748748	0.830145	0.817481	0.913577	0.903173	0.917095	0.984984
Covid6	0.742821	0.996802	0.729478	0.923428	0.797805	0.960638	0.951514	0.865538	0.99259
Covid7	0.72543	0.984191	0.667671	0.827951	0.764797	0.924376	0.885108	0.931836	0.986085
Covid8	0.833449	0.999798	0.70832	0.886624	0.878143	0.886901	0.887842	0.797795	0.969047
Covid9	0.762323	0.837926	0.658449	0.781237	0.810642	0.975449	0.975839	0.925519	0.996357
Covid10	0.827891	0.958029	0.750192	0.903324	0.849761	0.913873	0.912715	0.919398	0.989518
Mean Value	0.7873	0.9486	0.7174	0.8497	0.8219	0.9280	0.9211	0.8824	**0.9858**

Table 2 clearly highlights the performance of different methods in preserving brightness. RSWHE emerges as the leading method in this regard, with MMBEBHE following closely in second place based on AMBE.

Furthermore, Table 3 presents the Structural Similarity Index (SSIM) values compared to the original image, utilising SSIM to effectively assess the image's smoothness. The results clearly demonstrate the strengths of these methods in enhancing image quality. RSWHE again performs the best, while AHE comes second among the others in terms of SSIM.

V. CONCLUSION

This paper presents a comparative study of different histogram equalization-based image enhancement methods, specifically HE, AHE, CLAHE, BBHE, DSIHE, RMSHE, RSIHE, MMBEBHE, and RSWHE, applied to COVID-19 positive CXR images. The CXR images were sourced from Kaggle for this analysis. Upon evaluating the experimental results through metrics such as PSNR, brightness preservation (AMBE), and structural similarity index (SSIM), we observed that HE, BBHE, and DSIHE did not perform well. In contrast, the other methods exhibited better performance. Notably, RSWHE demonstrated the highest levels of PSNR, brightness preservation, contrast enhancement, and structural similarity index compared to all other approaches. Our findings indicate that substantial progress has been made in this area; however, considerable potential remains for future research, particularly in enhancing medical imaging techniques.

References

[1] P. Zhai, Y. Ding, X. Wu, J. Long, Y. Zhong, and Y. Li, “The epidemiology, diagnosis and treatment of COVID-19 Pan,” *Int. J. Antimicrob. Agents*, vol. 55, pp. 1–14, 2020.

[2] D. L. Weiner, V. Balasubramaniam, S. I. Shah, and J. R. Javier, “COVID-19 impact on research, lessons learned from COVID-19 research, implications for pediatric research,” *Pediatr. Res.*, vol. 88, no. 2, pp. 148–150, 2020, doi: 10.1038/s41390-020-1006-3.

[3] I. Goel, S. Sharma, and S. Kashiramka, “Effects of the COVID-19 pandemic in India: An analysis of policy and technological interventions,” *Heal. Policy Technol.*, vol. 10, no. 1, pp. 151–164, 2021, doi: 10.1016/j.hlpt.2020.12.001.

[4] X. Mei *et al.*, “Artificial intelligence-enabled rapid diagnosis of patients with COVID-19.,” *Nat. Med.*, vol. 26, pp. 1224–1228, 2020, doi: 10.1038/s41591-020-0931-3.

[5] J. Bullock, A. Luccioni, K. H. Pham, C. S. N. Lam, and M. Luengo-Oroz, “Mapping the Landscape of Artificial Intelligence Applications against COVID-19,” *J. Artif. Intell. Res.*, vol. 69, pp. 807–845, 2020.

[6] K. K. Singh, M. Siddhartha, and A. Singh, “Diagnosis of coronavirus disease (COVID-19) from chest X-ray images using modified XceptionNet,” *Rom. J. Inf. Sci. Technol.*, vol. 23, no. June, pp. S91–S115, 2020.

[7] K. El Asnaoui and Y. Chawki, “Using X-ray images and deep learning for automated detection of coronavirus disease,” *J. Biomol. Struct. Dyn.*, vol. 0, no. 0, pp. 1–12, 2020, doi: 10.1080/07391102.2020.1767212.

[8] H. Benbrahim, H. Hachimi, and A. Amine, “Deep Transfer Learning with Apache Spark to Detect COVID-19 in Chest X-ray Images,” *Rom. J. Inf. Sci. Technol.*, vol. 23, no. S, pp. S117–S129, 2020.

[9] I. D. Apostolopoulos, S. I. Aznaouridis, and M. A. Tzani, “Extracting Possibly Representative COVID-19 Biomarkers from X-ray Images with Deep Learning Approach and Image Data Related to Pulmonary Diseases,” *J. Med. Biol. Eng.*, vol. 40, no. 3, pp. 462–469, 2020, doi: 10.1007/s40846-020-00529-4.

[10] M. A. C. Huergo and N. T. K. Thanh, “Current advances in the detection of COVID-19 and evaluation of the humoral response,” *Analyst*, vol. 146, no. 2, pp. 382–402, 2021, doi: 10.1039/d0an01686a.

[11] R. Zill-e-Huma and A. Wilkinson, "Treatment Strategies for COVID-19 in Pregnancy: Short Review of Current Recommendations," *Open J. Obstet. Gynecol.*, vol. 11, no. 07, pp. 823–829, 2021, doi: 10.4236/ojog.2021.117076.

[12] R. D. Ekta, "Computer-Aided Diagnosis (CAD) for Chest X-Rays Using Artificial Intelligence : An Overview," *J. Emerg. Technol. Innov. Res.*, vol. 9, no. 3, pp. g802–g808, 2022.

[13] J. D. Lopez-Cabrera, R. Orozco-Morales, J. A. Portal-Diaz, O. Lovelle-Enriquez, and M. Perez-Diaz, "Current limitations to identify COVID-19 using artificial intelligence with chest X-ray imaging," *Health Technol. (Berl).*, vol. 11, pp. 411–424, 2021, doi: 10.1007/s12553-021-00520-2.

[14] B. G. S. Cruz, J. Sölter, M. N. Bossa, and A. D. Husch, "On the Composition and Limitations of Publicly Available COVID-19 X-Ray Imaging Datasets," *arXiv:2008.11572v1*, pp. 1–12, 2020.

[15] W. Huda and R. Brad Abrahams, "X-ray-based medical imaging and resolution," *Am. J. Roentgenol.*, vol. 204, no. 4, pp. W393–W397, 2015, doi: 10.2214/AJR.14.13126.

[16] N. O. R. H. Saad, N. O. R. Ashidi, M. A. T. Isa, A. Amer, and M. Salih, "Local Neighbourhood Image Properties for Exposure Region Determination Method in Nonuniform Illumination Images," pp. 79977–79997, 2020, doi: 10.1109/ACCESS.2020.2990730.

[17] E. A. B. da Silva and G. V. Mendonca, *Digital Image Processing*. 2004.

[18] S. M. P. Etta D. Pisano, Shuquan Zong, Bradley M. Hemminger, Marla Deluca, R. Eugene Johnston, Keith Muller, M. Patricia Braeuning, "Contrast Limited Adaptive Histogram Equalization Image Processing to Improve the Detection of Simulated Spiculations in Dense Mammograms," *Journalof Digit. Imaging*, vol. 11, no. 4, pp. 193–200, 1998, doi: 10.1587/transinf.2016EDL8049.

[19] Y. T. Kim, "Contrast enhancement using brightness preserving bi-histogram equalization," *IEEE Trans. Consum. Electron.*, vol. 43, no. 1, pp. 1–8, 1997, doi: 10.1109/30.580378.

[20] Y. Wang, Q. Chen, and B. Zhang, "Image enhancement based on equal area dualistic sub-image histogram equalization method," *IEEE Trans. Consum. Electron.*, vol. 45, no. 1, pp. 68–75, 1999, doi: 10.1109/30.754419.

[21] S. Der Chen and A. R. Ramli, "Contrast enhancement using recursive mean-separate histogram equalization for scalable brightness preservation," *IEEE Trans. Consum. Electron.*, vol. 49, no. 4, pp. 1301–1309, 2003, doi: 10.1109/TCE.2003.1261233.

[22] K. S. Sim, C. P. Tso, and Y. Y. Tan, "Recursive sub-image histogram equalization applied to gray scale images," *Pattern Recognit. Lett.*, vol. 28, no. 10, pp. 1209–1221, 2007, doi: 10.1016/j.patrec.2007.02.003.

[23] S. Der Chen and A. R. Ramli, "Minimum mean brightness error bi-histogram equalization in contrast enhancement," *IEEE Trans. Consum. Electron.*, vol. 49, no. 4, pp. 1310–1319, 2003, doi: 10.1109/TCE.2003.1261234.

[24] M. Kim and M. G. Chung, "Recursively separated and weighted histogram equalization for brightness preservation and contrast enhancement," *IEEE Trans. Consum. Electron.*, vol. 54, no. 3, pp. 1389–1397, 2008, doi: 10.1109/TCE.2008.4637632.